Irreversibility line in $YBa_2Cu_3O_7$ thin films: Correlation of transport and magnetic behavior

J. Deak and M. McElfresh*
Physics Department, Purdue University, West Lafayette, Indiana 47907

John R. Clem and Zhidong Hao†
Ames Laboratory and Department of Physics and Astronomy, Iowa State University, Ames, Iowa 50011

M. Konczykowski
Laboratoire des Solides Irradiés, École Polytechnique, 91128 Palaiseau, France

R. Muenchausen, S. Foltyn, and R. Dye
Superconductivity Technology Center, Los Alamos National Laboratory, Los Alamos, New Mexico 87545
(Received 14 January 1993; revised manuscript received 20 July 1993)

Using magnetic and magnetotransport measurements, we show that a $YBa_2Cu_3O_7$ thin-film sample has a single irreversibility line (IRL), which is the same as the vortex-glass-transition phase boundary. Results suggest that the effects of pinning persist above the glass-transition temperature T_g, and that it is the loss of critical-current density J_c rather than an onset of reversible magnetic behavior that characterizes the vortex-glass transition. Measurements of dc magnetization are shown to confirm a theoretical model that explains why the determination of T_g requires that field-cooled data be collected on cooling (FCC) rather than on warming (FCW), as is frequently done. The use of the ac susceptibility response for measuring T_g is shown to be a valid measure only at low frequency. This is because both the fundamental-frequency and third-harmonic ac susceptibilities measure the onset of ac flux penetration rather than the onset of irreversibility. The frequency dependence of the onset temperature of ac flux penetration (T_{on}) is shown to follow the vortex-glass-model dependence $T_{on}=C(2\pi f)^{[1/[(z-1)\nu]]}+T_g$, with values of z and ν consistent with those determined from scaling of the magnetotransport data.

I. INTRODUCTION

The first observation of the so-called "irreversibility line" (IRL) in high-temperature superconductors was that of Müller, Tagashige, and Bednorz on a polycrystalline sample of $(La_{2-x}Ba_x)CuO_4$.[1] They used a dc magnetic method that has become one of the standard methods for measuring the IRL. The IRL they determined was a curve with a dependence $B\sim(1-t)^{3/2}$, where the reduced temperature $t=T/T_c$. Since this dependence was the same as that characterizing spin-glass transitions, the transition was by analogy referred to as a vortex-glass transition. Various models were put forward to describe this crossing from irreversible to apparently reversible magnetic behavior. The first of these models treated the ceramic superconductor as an agglomeration of separate superconducting grains connected by a grain-boundary phase, which results in superconducting weak links between grains.[2,3]

Other competing explanations[4,5] for the IRL were later presented, including a model based on flux creep.[6] When the properties that had been attributed to the polycrystalline nature of the materials also were observed in single crystals, the flux-creep interpretation of the IRL found favor. In the flux-creep model, the IRL is not a thermodynamic phase transition, but rather a dynamic crossover resulting from the crossing from a regime in which the system response is flux-flow dominated to one that is pinning dominated. Further apparent support for this model came from the time dependence of the magnetization,[7] the frequency dependence of the IRL when measured by ac susceptibility (χ_{ac}),[8] and the Arrhenius dependence of the resistivity.[9] The flux-creep model also predicts that a linear resistivity exists in the limit of zero current density.

The early measurements of voltage as a function of current (V-I) on thin films of $YBa_2Cu_3O_{7-\delta}$ (YBCO) showed a behavior that could be described by the flux-creep model.[10] This study also showed that the pinning potential energy U had a current density (J) dependence described by $U\propto\ln(J_c/J)$, where J_c is the critical-current density. This dependence has been confirmed by more recent magnetic measurements.[11] Other models that could account for this $U(J)$ dependence were put forward, including the collective-flux-creep model of Feigel'man *et al.*[5] In addition to $U(J)$, their theory was able to account for long- and short-term relaxation results[12] and the temperature dependence of the critical-current density (J_c).[13,14] More recent V-I measurements have shown that the positive-curvature flux-creep-type V-I behavior observed earlier[10] can give way at lower temperatures to a region of negative curvature.[15] Associated with this negative curvature is a disappearance of the linear resistivity resulting from the divergence of U in the small-J limit. The models that predict this crossover in V-I behavior are the model of Feigel'man *et al.* and the

vortex-glass model of Fisher, Fisher, and Huse.[4] Their models, like other models describing a transition of the vortex lattice into a glassy state, consider the IRL to be a thermodynamic phase transition rather than a dynamic crossover. The confirmed disappearance of the linear resistivity greatly improves the prospects for application of these superconductors.

Several methods have been used to measure the IRL, and as a result, several definitions for the IRL have emerged. It is our contention that for the case of YBCO thin films of sufficient thickness, there is only one IRL and it is the same as T_g measured by transport. Here we present results of various IRL measurement methods. The first measurement of the IRL, by Müller, Tagashige, and Bednorz using dc magnetization measurements, seemed to provide a reliable method.[1] However, we will show that a commonly used variation of this method does not provide reliable results. The use of fundamental-frequency ac susceptibility (χ_1) became a popular method to measure the IRL, even after the warnings of Shaulov and Dorman.[16] More recently, the realization that χ_1 is a measure of ac flux penetration[17–19] rather than irreversibility has led many to choose the third-harmonic ac susceptibility response to determine the IRL. The basis for using this method is that the existence of irreversibility will produce harmonics.[20] However, we will show that there is actually a coincidence of both the fundamental and third-harmonic response onsets which results from ac flux penetration occurring in a region in which the current-voltage behavior is nonlinear.

II. EXPERIMENTAL DETAILS

Epitaxial YBCO thin films, with the c axis perpendicular to the film plane, were prepared by pulsed laser deposition onto heated (001) $LaAlO_3$ substrates using a method described previously.[21] The superconducting transition temperatures (T_c) ranged from 89.8 to 90.3 K, and the transition width ΔT_c was about 2 K as measured by ac susceptibility at 2.5 MHz. Measurements of the voltage as a function of current (V-I), ac susceptibility (χ_{ac}), and dc magnetization as a function of temperature were made on the same thin-film sample using procedures described previously.[22] The χ_{ac} measurements include the in- and out-of-phase responses at the fundamental and the third-harmonic frequencies. Three different types of dc magnetization measurements were made. These included zero-field cooled (ZFC) "field cooled with data collected on warming" (FCW), and "field cooled with data collected on cooling" (FCC).

III. RESULTS AND DISCUSSION

A. Transport

Figure 1 is a plot of electric field E versus current density J for a 3000-Å-thick film in an applied magnetic field $H=30$ kOe. Similar data sets were collected at various values of H. The electric field is determined using the relation $E=V/L$, where V is the measured voltage and L is the length of the film bridge. The current density is determined using the relation $J=I/A$, where A is the cross-sectional area of the film bridge. The E-J curves are isotherms, ranging in 1-K increments from 70 K at the lower right to 89 K at the upper left. Three regions of differing curvature can be distinguished. At the highest temperatures, an Ohmic region is evident. As the temperature is decreased, a positive-curvature region develops, with individual isotherms in this region showing a crossing from Ohmic to power-law behavior as the current increases. The temperature of crossing from Ohmic-behavior isotherms to positive-curvature isotherms is denoted as T_{Ohm} (dot-dashed line). As the temperature is decreased further, the E-J curvature becomes negative. The temperature of crossing from positive to negative-curvature isotherms is denoted T_g (dashed line).

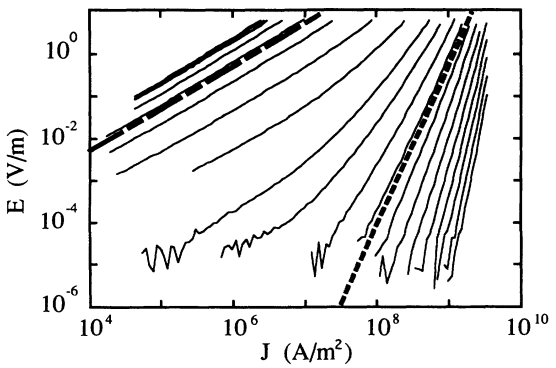

FIG. 1. Plots of ln$E$ vs ln$J$ for a 3000-Å YBCO thin film in an applied magnetic field $H=30$ kOe. Each curve is an isotherm, ranging from 70 K at the lower right to 89 K at the upper left, in increments of 1 K. The dot-dashed line at higher temperatures identifies the isotherm $E(J, T=T_{Ohm}=84.8$ K), while the dashed line is the glass transition isotherm, $E(J, T=T_g=77.8$ K) determined from scaling the E-J results.

Values of T_{Ohm} at various applied fields are plotted in Fig. 2. These values fall below the H_{c2} curve (T_{c2}) that was estimated using the measured transition temperature (at $H=0$) for the film in combination with prior determinations of H_{c2} on YBCO crystals.[23] As a result of experimental limits on J and E, T_{Ohm} is defined as the lowest temperature for which an E-J isotherm is Ohmic to the highest observed current density. The resistivity of the T_{Ohm} isotherms was found to be roughly 50 $\mu\Omega$ cm at all fields. It is observed that the Ohmic region above T_{Ohm} curve in Fig. 2 has completely reversible dc magnetic behavior. The transport behavior in this region of the E-J curves is due to thermally enhanced flux flow.

Below T_{Ohm} and above T_g, the E-J behavior (Fig. 1) is characteristic of thermally activated flux motion and manifests a crossing from Ohmic behavior at small J to power-law behavior at larger J values, with a nonzero linear resistance at all J. Recent results support the idea that thermal fluctuations enhance flux flow also in this region of E-J behavior.[24] Even though there is a linear component in the E-J behavior of this regime, it is not necessary that the $M(H)$ behavior be reversible, except in the small E-J limit, where the E-J behavior is Ohmic. Measurements on a sufficiently long time scale do show

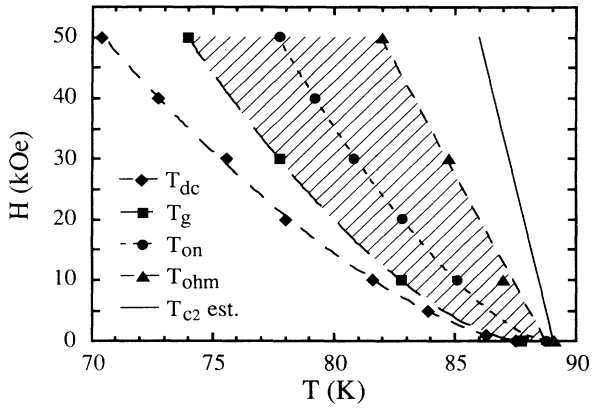

FIG. 2. "Irreversibility line" as determined by several methods on the same 3000-Å thick YBCO film. Included are lines determined by dc magnetization (T_{dc}), third-harmonic χ_{ac} (T_{on}), and E-J magnetotransport (T_g) measurements. The line defining T_{c2} is an estimate determined from earlier measurements on single crystals and the line identified as T_{Ohm} is the point above which the E-J curves are always Ohmic. The hatched region indicates the portion of the phase diagram above T_g where a E-J scaling is expected.

evidence of reversible behavior resulting from the resistive decay of J into the Ohmic portion of the E-J curve. On the other hand, in the case of single crystals the crossing from purely Ohmic to purely power-law behavior has been used to define the IRL.[25]

Within the model of Anderson and Kim,[26] E can be expressed in the thermally activated flux motion regime in a general form[27] as

$$E(J,T)=2\rho_0 J_c \exp\left[\frac{-U}{k_B T}\right]\sinh\left[\frac{JU}{J_c k_B T}\right], \quad (1)$$

where J_c is the critical current density at $T=0$, $U(B,T)$ is the activation energy for flux jumps, and $\rho_0(B,T)$ is the resistivity at $J=J_c$. Two limiting behaviors, which can be solved exactly for some geometries, can be distinguished. The thermally activated flux-flow (TAFF) regime is observed at low driving currents, $J \ll J_c k_B T/U$, where the sinh term may be replaced by its argument.[28] The resistivity is then given by

$$\rho_{TAFF}=\frac{E}{J}=\frac{2\rho_0 U}{k_B T}\exp\left[\frac{-U}{k_b T}\right]. \quad (2)$$

Note that there is no J dependence so that this describes a regime with Ohmic behavior. When $U/k_B T \gg 1$ and J is very close to J_c, backwards hopping of the vortices may be neglected, and the sinh term may be replaced by an exponential. The resistivity may then be expressed as

$$\rho=\frac{E}{J}=\rho_0\frac{J_c}{J}\exp\left[\frac{U}{k_B T}\left[\frac{J}{J_c}-1\right]\right]. \quad (3)$$

This is known as the flux-creep regime. This flux-creep resistivity describes a non-Ohmic regime, since it has a J dependence. Equation (3) predicts exponential behavior at large current densities. However, as seen in Fig. 1 and observed previously, this region experimentally shows power-law behavior at large current densities. In fact, it has been reported that U depends on J as $U(J)=U_J\ln(J_0/J)$, where J_0 is the current density at which U approaches zero. When this is substituted into Eq. (1), it is found that ρ is dominated by power-law behavior, which frequently is observed.[10,27] Since flux creep is indicative of vortex pinning, this suggests that vortex pinning exists in the region between T_{Ohm} and T_g. The linearity of the low-J part of the E-J isotherms in this region is indicative of an exponential creep rate, but the actual relaxation behavior is probably much more complicated than this,[28] and it may be too large to measure accurately.

For a superconductor containing sufficient disorder, recent vortex-glass-transition models describe a continuous phase transition from a vortex-liquid state above T_g into a vortex-glass state.[4,5] As in Fig. 1, these models predict that below T_g the E-J behavior will have a negative curvature that results from the divergence of the pinning potential U in the small-current-density limit. In this regime, the activation energy for a volume of the vortex lattice to jump diverges as $1/J^m$, for $0<m\leq 1$.[4] Because of this divergence, the vortices become rigidly pinned, and the linear resistivity vanishes. The vortex-glass model of Fisher describes the J dependence of E at temperatures $T<T_g$ as

$$E \propto \exp\left[-\left[\frac{J_c}{J}\right]^m\right], \quad (4)$$

where m is a universal exponent.[4] This equation shows negative curvature in a log-log plot. Since the linear resistance goes to zero, it is possible for supercurrents to persist indefinitely. Now, however, rather than having a logarithmic time dependence, which follows from the Anderson-Kim E-J form [Eq. (3)], the creep behavior is predicted to be nonlogarithmic in time.[4] This nonlogarithmic creep behavior has been observed in both crystals[12] and films[29] of YBCO.

The vortex-glass-transition model predicts that the data above and below T_g can be scaled onto separate universal curves.[4] The following scaling relations were used to determine T_g:

$$V/I \sim |T-T_g|^{\nu(z-1)} \text{ and } I \sim |T-T_g|^{2\nu}. \quad (5)$$

For a three-dimensional transition, it is expected that $z>4$ and $1<\nu<2$.[15] Figure 3 is typical of our scaled data, but note that the axes have been expressed in terms of ρ and J, which differ from Eq. (3) by constants and thus have no effect on the scaled parameters. The E-J data scale for the values z and ν that are listed in Table I. There is a margin of error (± 1 K) in the determination of T_g resulting from the difficulty in determining the isotherm where the curvature changes from positive to negative. As observed previously in thin films,[15] these E-J curves scale over a wide temperature range, which broadens with increasing field. Shown in Fig. 3 are the 10-kOe E-J data, which scale for up to about 5 K above T_g. The region over which scaling is observed is represented by the hatched area in Fig. 2. It is found that E-J data taken at 50 kOe scale up to about 8 K above T_g.

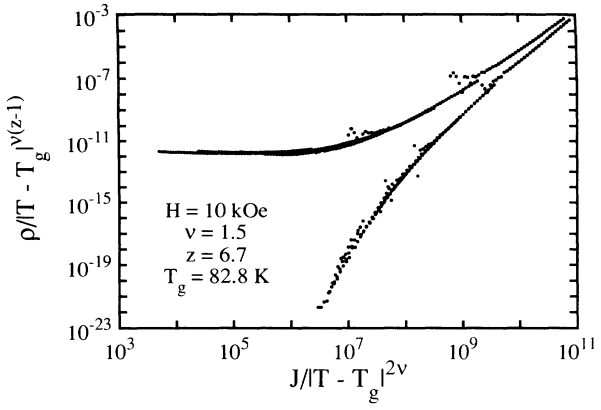

FIG. 3. *E-J* curves at 10 kOe scaled to $V/I \sim |T-T_g|^{\nu(z-1)}$ and $I \sim |T-T_g|^{2\nu}$. The temperatures of the curves scaled ranged from 87 to 75 K and a value $T_g = 82.8$ K was determined.

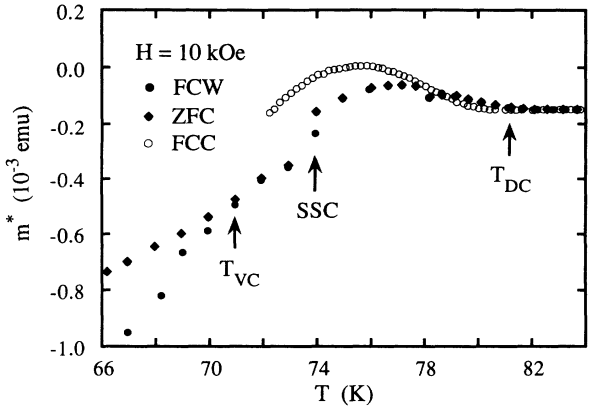

FIG. 4. Typical dc magnetization curves for zero-field-cooled (ZFC), field-cooled with data collected on warming (FCW), and field-cooled with data collected on cooling (FCC) methods. At T_{vc} and above, the ZFC and FCW curves are coincident, while only at T_{dc} does the FCC curve become coincident with the other two. The sample is the same 3000-Å thin film of YBCO measured at $H = 10$ kOe. SSC identifies an experimental artifact described in the text.

All of the curves in the *E-J* data for $T < T_g$ scale reasonably well. The dashed line in Fig. 1 is a plot of $E(J, T = T_g)$ using the parameters z and T_g determined at 30 kOe. For a three-dimensional glass transition, the *E-J* curve at T_g may be expressed as $E(J, T = T_g) = KJ^{(z+1)/2}$, where z is a constant determined from scaling.[4] The values of T_g determined at various applied fields by scaling are those plotted in Fig. 2.

Although the *E-J* curves allow for the most accurate determination of the IRL, other methods that are much simpler to perform, such as dc magnetization and ac susceptibility, have been used for this purpose. Measuring *E-J* behavior is not only time consuming, but also complicated by the need to make low-resistance Ohmic contacts. In spite of these shortcomings, *E-J* measurements provide detailed information on the electromagnetic behavior of the superconductor.

B. dc magnetization

The results of dc magnetization measurements on the 3000-Å-thick film are shown in Fig. 4. The curves in Fig. 4 correspond to three different types of measurements: (1) zero-field cooled (ZFC), (2) field cooled with data collected on warming (FCW), and (3) field cooled with data collected on cooling (FCC). For both the ZFC and FCW curves, there is a distinctive negative change in the apparent magnetization at a point we will denote T_{dc}. The large values of this magnetization and the anomalous superconducting quantum interference device (SQUID) output signals below this point are consistent with the disappearance of irreversibility at T_{dc}.[30] As shown in Fig. 4 at $H = 10$ kOe, the ZFC and FCW curves are coincident from T_{dc} down to T_{vc} where they split into two separate curves. On the other hand, as the temperature is decreased from above T_{dc}, the FCC curve initially makes a negative deviation at T_{dc} before turning positive. The FCC curve does not coincide with the FCW and ZFC curves except at T_{dc} and above. The model of Clem and Hao predicts this general behavior.[31]

There are several technical considerations that complicate the use of dc magnetometer measurements. First, dc magnetometers are designed to measure samples with homogeneous magnetization, which is not always true of superconducting samples with strong pinning. The result of this inhomogeneous magnetization is that the signal observed is not of the point-dipole form that the instrument was designed to analyze. In these cases the quantitative accuracy (and even the sign) of the measurement must be questioned. However, these results can have value if used to observe relative changes. The point labeled SSC in Fig. 4 is an artifact related to the inability of the signal analysis procedure to properly fit the SQUID output. Steps like the one at SSC occur when the SQUID amplifier range is changed during measurement. Another unrelated technical consideration is associated with the motion of the sample during measurement. Because the sample is moved (cycled) during measurement, it is possible to cycle the sample through minor hysteresis loops unless the motion (scan length) is limited to a region of the applied magnetic field that is spatially homogeneous. This effect becomes more pronounced as the field is increased. The value of T_{dc} will be scan-length dependent at higher applied fields unless a sufficiently short scan length is used. The same value for T_{dc} was determined for scan lengths of 3.0 cm and shorter. A determination of the IRL using the ZFC-FCC method with scan length

TABLE I. Parameters ν, z, and T_g at various magnetic fields as determined by scaling of the *E-J* data to $V/I \sim |T-T_g|^{\nu(z-1)}$ and $I \sim |T-T_g|^{2\nu}$.

H (kOe)	z	ν	T_g (K)
10	6.7	1.5	82.8
30	6.8	1.6	77.8
50	6.8	1.7	74.0

of 2.5 cm is presented in Fig. 2. Note that the curve determined using this method falls close to, but below, the curve for T_g determined by transport measurements. The resolution of the measurement is about 1×10^{-6} emu, which corresponds to about 5 A/cm^2.

The FCW method, in which one determines the temperature where the FCW and ZFC magnetization curves split, does *not* in general permit an accurate determination of the irreversibility line. To show why this is so, it is of interest to make a detailed comparison of the flux-density profiles for three distinct cases: FCC (field-cooled magnetization, with data collected as the sample is gradually *cooled* in an applied magnetic field), FCW (field-cooled magnetization, with data collected as the sample is gradually *warmed* in an applied magnetic field), and ZFC (zero-field-cooled magnetization, with data collected as the sample is gradually warmed in an applied magnetic field). The differences may be most clearly understood by considering the behavior of a long superconducting cylinder (radius R) in a parallel magnetic field H_0, using standard critical-state theory to account for the flux density (B) and temperature dependence of $J_c(B,T)$ and $B_{eq}(H_0,T)$ [or $M_{eq}(H_0,T)$].

During a FCC magnetization measurement, the flux density at the surface drops, as it attempts to remain in equilibrium with the externally applied field. This leads to gradual flux expulsion. At each temperature point, the sample has a flux-density profile in which, as a function of distance ρ from the center, the local flux density $B(\rho)$ *decreases* monotonically out to the surface. To illustrate this with a simple example, let us assume that the critical-state profiles of $B(\rho,T)$ versus ρ can be calculated from $dB/d\rho=\pm(4\pi/c)J_c(T)$, where J_c is independent of B, but is a monotonically decreasing function of T. (We assume relatively weak pinning, such that the flux-trapping depth[32] is always larger than R.) The temperature T_{dc} is the temperature above which $J_c(T)$ is effectively zero. We define $T_{c1}(H_0)$ and $T_{c2}(H_0)$ as the temperatures T at which $H_{c1}(T)=H_0$ and $H_{c2}(T)=H_0$, respectively. Shown in Fig. 5 are the resulting flux-density profiles $B(\rho,T)$ for successively decreasing temperatures during field cooling: $T\geq T_{cz}$ (curve *a*), $T_{dc}\leq T\leq T_{c2}$ (curve *b*), $T_{c1}<T<T_{dc}$ (curves *c* and *d*), and $T\leq T_{c1}$ (curve *e*). At each temperature the value of $B(R,T)=B_{eq}(H_0,T)$, and the slope of the B-ρ curve is $-(4\pi/c)J_c(T)$. At temperatures $T_{dc}\leq T<T_{c2}$, this slope is zero, but as T drops below T_{dc} the critical-state slope becomes steeper. Note that $B(R,T_{c2})=H_0$ (Fig. 5, curve *a*) because $H_0=H_{c2}$ when $T=T_{c2}$ and that $B(R,T_{c1})=0$ (Fig. 5, curve *f*) because $H_0=H_{c1}$ at $T=T_{c1}$.

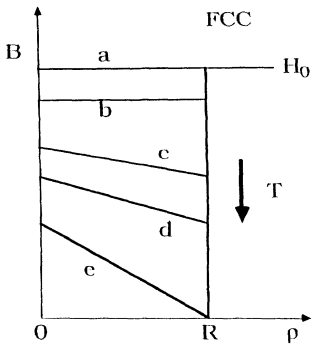

FIG. 5. Sketch of the FCC flux-density profiles $B(\rho,T)$ vs distance ρ from the center of the cylinder, for decreasing temperatures during field cooling: $T\geq T_{c2}$ (curve *a*), $T_{dc}\leq T<T_{c2}$, (curve *b*), $T_{c1}<T<T_{dc}$ (curves *c* and *d*), and $T\leq T_{c1}$ (curve *e*).

Shown in Fig. 6 are flux-density profiles $B(\rho,T)$, sketched for successively increasing temperatures during a FCW magnetization measurement: $T\leq T_{c1}$ (curve *a*), $T_{c1}<T<T_{vc}$ (curves *b* and *c*), $T=T_{vc}$ (curve *d*), $T_{vc}<T<T_{dc}$ (curve *e*), $T_{dc}\leq T<T_{c2}$ (curve *f*), and $T>T_{c2}$ (curve *g*). During a FCW measurement, only at the lowest temperatures $T\leq T_{c1}$ [compare Figs. 6 (curve *a*) and 5 (curve *e*)] does the flux-density profile decrease monotonically out to the surface. As the temperature increases above T_{c1} (Fig. 6, curves *b* and *c*) the flux density at the surface increases, and a flux-density front (having a higher flux density at the surface than at some point farther in) advances inward. The flux-density profile $B(\rho)$ has a V-shaped minimum at some radial coordinate ρ_v, where $0<\rho_v<R$. The slope $dB/d\rho=(4\pi/c)J_c(T)$ for $\rho>\rho_v$, where magnetic flux is moving inward, and $dB/d\rho=-(4\pi/c)J_c(T)$ for $\rho<\rho_v$, where flux is moving outward. At temperature T_{vc} (Fig. 6, curve *d*), the V-shaped minimum in $B(\rho)$ just touches the center of the sample ($\rho_v=0$). For temperatures $T_{vc}<T<T_{dc}$ (Fig. 6, curve *e*), the local flux density *increases* monotonically out to the surface, and flux continuously enters the sample as the temperature rises. The slope of the flux-density profile decreases and eventually becomes perfectly flat at T_{dc} (Fig. 6, curve *f*). At temperatures $T\geq T_{c2}$ (Fig. 6, curve *g*), bulk superconductivity is quenched, and $B(\rho)=H_0$.

Shown in Fig. 7 are flux-density profiles $B(\rho,T)$, sketched for successively increasing temperatures during a ZFC magnetization measurement: $T\leq T_{c1}$ (curve *a*), $T_{c1}<T<T_{dc}$ (curves *b*–*e*), $T_{dc}\leq T<T_{c2}$ (curve *f*), and $T\geq T_{c2}$ (curve *g*). Initially, $B(\rho,T)=0$ for all temperatures below T_{c1} (Fig. 7, curve *a*). As the temperature rises above T_{c1}, however, a flux-density front [having a

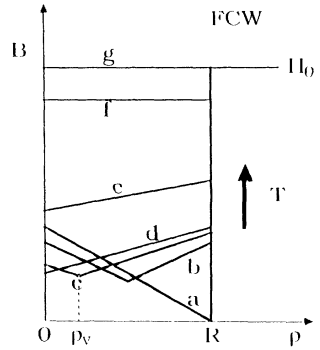

FIG. 6. Sketch of the FCW flux-density profiles $B(\rho,T)$ vs distance ρ from the center of the cylinder, sketched for increasing temperatures: $T\leq T_{c1}$ (curve *a*), $T_{c1}<T<T_{vc}$ (curves *b* and *c*), $T=T_{vc}$ (curve *d*), $T_{vc}<T<T_{dc}$ (curve *e*), $T_{dc}\leq T<T_{c2}$ (curve *f*), and $T\geq T_{c2}$ (curve *g*).

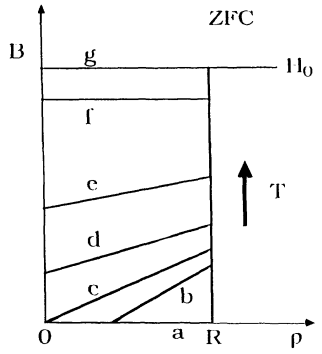

FIG. 7. Sketch of the ZFC flux-density profiles $B(\rho,T)$ vs distance ρ from the center of the cylinder, sketched for increasing temperatures: $T \leq T_{c1}$ (curve *a*), $T_{c1} < T < T_{dc}$ (curves *b*–*e*), $T_{dc} \leq T < T_{c2}$ (curve *f*), and $T \geq T_{c2}$ (curve *g*).

higher flux density at the surface than at some point farther in, with slope $dB/d\rho = (4\pi/c)J_c(T)$] appears at the surface (Fig. 7, curve *b*), and its advances inward as the temperature gradually increases. At some temperature (Fig. 7, curve *c*) this flux-density front reaches the center of the sample. As the temperature further increases, the slope of the flux-density profile decreases (Fig. 7, curves *d* and *e*), eventually becoming perfectly flat at T_{dc} (Fig. 7, curve *f*). Note that the flux-density profiles for FCW and ZFC are identical for temperatures $T \geq T_{vc}$ (curves *d*, *e*, and *f* in Figs. 6 and 7). Thus the magnetization curves for the two processes must be identical for $T \geq T_{vc}$. It is clear, however, that T_{vc} has nothing to do with the irreversibility temperature, since the joining of the magnetization curves at T_{vc} follows from the critical-state model, which is describing the irreversibility of the sample.

Shown in Fig. 8 is a sketch of the resulting FCC, FCW, and ZFC magnetization curves. Because the flux-density profiles are frozen in at temperatures below T_{c1}, the magnetization versus temperature is flat in this temperature range. In the temperature range $T_{c1} < T < T_{dc}$, where the critical-current density obeys $J_c > 0$, the critical-state

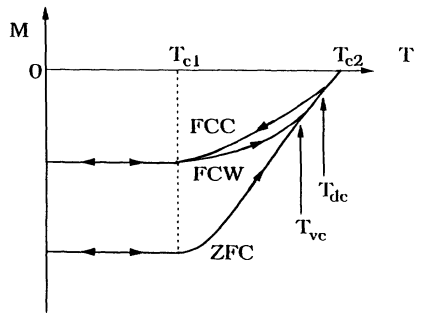

FIG. 8. Sketch of the FCC, FCW, and ZFC magnetizations vs temperature *T*. The FCC and ZFC magnetization curves separate below T_{dc} [Figs. 5 (curve *b*) and 7 (curve *f*)], which we identify as the vortex-glass transition temperature. The FCW and ZFC magnetization curves, however, separate below T_{vc} (Fig. 6, curve *d*), an effect that has nothing to do with the irreversibility temperature, since it occurs even when J_c is large.

model requires that the FCC magnetization curve (which describes a flux density that everywhere has *negative* slope, as in Fig. 5) must lie above the FCW magnetization curve (which describes a flux density that has positive slope near the surface, as in Fig. 6). Only when $(4\pi/c)J_c(T)R$ is immeasurably small by comparison with H_0, i.e., only when $T \geq T_{dc}$, is the flux-density profile for all practical purposes flat. For such temperatures, the flux-density profiles for FCC, FCW, and ZFC all agree, and one is then measuring simply the reversible (equilibrium) magnetization curve. The FCW and ZFC curves separate only at temperatures below T_{vc}, while the FCC and ZFC curves separate only at temperatures below T_{dc}, which we identify as the vortex-glass transition temperature T_g.

An examination of Fig. 4 shows that, as predicted, the ZFC and FCW curves are superimposed to temperatures well below T_{dc}, while the FCC curve is only coincident with the ZFC curve above T_{dc}. Without further measurement, it is not possible to confirm that T_{dc} is an approximate determination of T_g. However, it would seem very likely to be so. At some point the magnetic moment associated with the irreversible magnetization falls below the resolution of the magnetometer, which will lead to an underestimate of the temperature where J_c disappears. Therefore a determination of the vortex-glass transition by dc magnetization measurements is expected to fall at a temperature lower than that determined by transport measurements.

C. Fundamental-frequency ac susceptibility

Shown in Fig. 9 is a plot of V_1' and V_1'', which are proportional to χ_1' and χ_1'', the in- and out-of-phase components of the fundamental-frequency (or first-harmonic) ac susceptibility, as a function of temperature for a

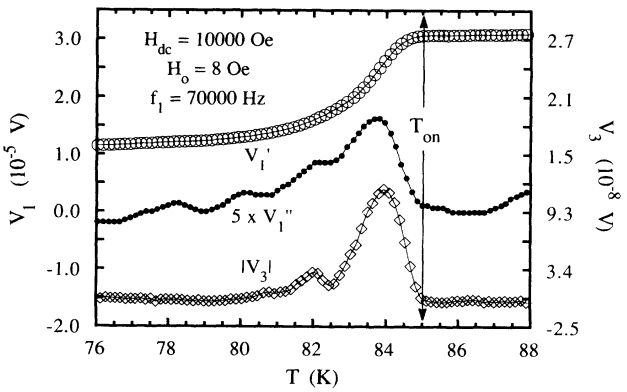

FIG. 9. Temperature dependence of voltages V_1' and V_1'', which are proportional to the in-phase (χ') and out-of-phase (χ'') components of the fundamental-frequency ac susceptibility. Also shown is the voltage $|V_3|$, which is proportional to the magnitude of the third-harmonic ac susceptibility $|\chi_3|$, as a function of temperature for the same 3000-Å thin film of YBCO. The fundamental frequency is 70 000 Hz, and ac amplitude $H_0 = 8$ Oe, and the applied dc field $H = 10$ kOe. The onset of the first and third harmonics occurs at the same temperature, which indicated by the arrows.

YBCO thin film. χ_1' and χ_1'' can be physically interpreted as measures of ac magnetic field screening and loss, respectively. This can be seen by considering a cylinder of radius R, composed of a conducting material that has been subjected to an oscillating magnetic field superimposed on a constant magnetic field parallel to the axis of the cylinder, $H=H_{dc}+h_0\cos(2\pi ft)$.[17] The time-dependent volume-averaged magnetic induction in the cylinder may be written

$$B=B_{dc}+b(t), \tag{6}$$

where

$$b(t)=h_0\cos(2\pi ft)+4\pi m(t) . \tag{7}$$

Since $m(t)$ is periodic in time with period $1/f$, it can be Fourier expanded in terms of frequency f and a complex harmonic susceptibility $\chi_n=\chi_n'+i\chi_n''$ as follows:

$$m(t)=h_0\sum_{n=1}^{\infty}[\chi_n'\cos(2\pi nft)+\chi_n''\sin(2\pi nft)] . \tag{8}$$

When the background signal is properly nulled, the measured voltage of an N-turn pickup coil wrapped around the cylinder is then

$$\begin{aligned}V(t)&=\frac{-N\pi R^2}{c}4\pi\frac{dm(t)}{dt}\\&=-4\pi h_0\frac{N\pi R^2}{c}\sum_{n=1}^{\infty}2\pi fn\{\chi_n''\cos(2\pi fnt)\\&\qquad-\chi_n'\sin(2\pi fnt)\} .\end{aligned} \tag{9}$$

A lock-in amplifier is typically used to separate these harmonic voltages, which are directly proportional to the harmonic susceptibilities. When the first harmonic is detected, the volume-averaged ac magnetic induction in the cylinder may be expressed in terms of χ_1' and χ_1'' as

$$\begin{aligned}b_1(t)&=h_0\cos(2\pi ft)+4\pi m_1(t)\\&=\mathrm{Re}\{[1+4\pi(\chi_1'+i\chi_1'')]h_0e^{-i2\pi ft}\} .\end{aligned}$$

This equation can be used to demonstrate that χ_1' is a measure of screening. When the cylinder is completely unscreened, $b_1(t)=h_0\cos(2\pi ft)$. For this to be true, $\chi_1'=\chi_1''=0$. In this case, the ac magnetic induction in the cylinder is large, but the induced screening current density J is small. Therefore losses are small. When the cylinder is completely screened, the ac magnetic field penetration depth $\delta=(c/2\pi)(\rho/f\mu)^{1/2}$, where μ is the permeability and ρ is the resistivity, is small. In this case, $b_1(t)=0$, so that $\chi_1'=-1/4\pi$ and $\chi_1''=0$. Losses will also be small in this case since the ac magnetic induction in the cylinder is small. Thus χ_1' is a measure of screening, and the more negative the value of χ_1', the greater the amount of screening. The onset temperature of ac magnetic screening (T_{on}) is shown in Fig. 9.

In the regime of incomplete screening, both J and the ac magnetic induction in the cylinder can become large, so that ac losses will be large. The energy loss per unit volume per cycle can be computed from $(1/4\pi)\int H\,dB$. When Eqs. (6) and (8) are used for B in this integral, the energy loss per unit volume per cycle is found to be $\pi h_0^2\chi_1''$. It is important to note that the higher harmonics of $m(t)$ do not contribute to this integral. Thus χ_1'' is a measure of loss. In general, losses are maximized when δ is on the order of some geometry-dependent length. χ_1'' will have a peak at the lowest temperature, T_p, where the ac magnetic induction has fully penetrated the sample. For the case of a long cylinder and an ac field applied parallel to its axis, it has been found that losses are maximized when $\delta=R/1.8$.[17] T_p is dependent on sample size, geometry, ρ, and f.

For a film patterned into a circle with radius R and the magnetic field applied normal to its surface, we estimate that T_p will occur at a value of the resistivity

$$\rho_{peak}\sim 2\pi^2\mu fRd/c^2 , \tag{10}$$

where d is the thickness of the film. This follows from setting the two-dimensional screening length Λ_f for an ac magnetic field perpendicular to the film's surface equal to R ($\Lambda_f=2\delta^2/d=R$). Thus T_p may be moved to different ρ values by varying f.

The above is true for normal metals.[17] For superconductors, however, both ρ and χ are dependent on the magnetic field. Since the resistivity of a superconductor is due to flux motion, ρ should be replaced with the flux-flow resistivity ρ_f and μ should be taken as the differential permeability in thermodynamic equilibrium.[17] The flux-flow skin depth is then represented as $\delta_f=(c/2\pi)(\rho_f/f\mu)^{1/2}$.

If pinning is present, then losses may be represented as $JE=E^2/\rho_f+J_cE$, where the first and second terms on the right-hand side represents losses due to flux flow and pinning, respectively.[33] When $E\gg\rho_fJ_c$, the above equations for flux penetration apply. If $E\ll\rho_fJ_c$, the peak in χ_1'' will still occur when the ac magnetic induction has penetrated to some geometry-dependent length, but the penetration depth L_p will have a frequency dependence that is small in comparison with its h_0 dependence. In this case, L_p will be proportional to h_0. For the specific case of a cylinder,[17] L_p is given by the condition

$$L_P=\frac{h_0c}{4\pi J_c} . \tag{11}$$

This crossover in the penetration depth to L_p occurs at low frequencies. This is because at low frequencies the ρ value required for the skin depth to be on the order of R [see Eq. (10)] occurs at a temperature below T_g, where pinning is strong.

In spite of the fact that T_p is actually a function of sample size and geometry, the measuring frequency, and the sample resistivity, it has been used by some to determine the IRL. The χ_1'' peak is *not* a direct measure of the onset of irreversible magnetic behavior. The fundamental frequency χ_{ac} response measures the extent to which an ac field has penetrated into the sample. At low f, T_p is more strongly dependent on h_0, and at high f, T_p is more strongly dependent on f. At intermediate f, the T_p dependence on h_0 and f is not well defined, and may be a complicated function of both h_0 and f.[17]

A schematic presentation of the dependencies of the χ_1'' peak is shown in Fig. 10.[34] When measuring the χ_{ac} response of a superconductor at high f, the position of the χ_1'' peak shifts to higher temperature as the measuring frequency is increased. In this case the peak (T_p) will occur at a temperature above the actual onset of irreversibility, T_g. This is the region to the right of T_g in Fig. 10. From Eq. (10), it can be seen that as f is increased, ρ_{peak} will increase; thus T_p must also increase. For sufficiently small values of ρ_{peak}, however, the penetration depth crosses to L_p as described above. This is the region shown to the left of T_g in Fig. 10. When this happens, T_p is less than T_g. The position of T_p in this regime will be dependent on L_p and thus on h_0 and J_c, as in Eq. (11). From Eq. (11) it can also be seen that if L_p is to remain on the order of R, J_c must increase as h_0 increases. Therefore, for small values of f, T_p shifts to lower temperature with increasing h_0.

It follows that T_p occurs at temperatures greater than T_g at high frequencies and at temperatures less than T_g at low frequencies. The dependence of the χ_1'' peak on f at higher frequencies and h_0 at lower frequencies makes it impossible to accurately determine T_g with a single temperature sweep at a single value of f and h_0. In order to approximate T_g using this method, it is necessary to take several temperature sweeps at constant H, while varying either f or h_0. In either case, it should be possible to determine T_g approximately by extrapolation. As will be discussed below, measuring T_{on} offers an alternative method for measuring T_g.

D. Third-harmonic ac susceptibility

The higher order harmonics of χ_{ac} have been used as a measure of the onset of irreversible magnetic behavior in various systems, including superconductors.[16,35] When the magnetic behavior of a material is completely reversible *and* the *E-J* relationship is linear, there will be no higher-order harmonics associated with χ_{ac}. However, when the *E-J* relationship is nonlinear, there will be a nonlinear *M-H* response and the generation of higher-order harmonics, whether the system is reversible or irreversible. When the magnetic behavior is irreversible, it follows that the *E-J* relationship must be nonlinear. As was shown by Bean, the odd harmonics of the hysteretic response of a superconductor in the critical state are always present.[20] The even harmonics will also be present if the hysteresis loop is asymmetric with respect to the origin.[35]

Shown in Fig. 9 are the voltages V_1' and $|V_3|$ proportional to both the in-phase part of the fundamental χ_{ac} response, χ_1', and the magnitude of the third-harmonic χ_{ac} response, $|\chi_3| = |\chi_3' + i\chi_3''|$, respectively, as a function of temperature measured using a fundamental frequency $f = 70\,000$ Hz in an applied dc field $H = 10$ kOe for the 3000-Å YBCO thin film. Clearly, as indicated in Fig. 9, both the fundamental and third-harmonic onsets are coincident. We have found a coincidence of the onsets of both the fundamental and third-harmonic χ_{ac} responses at fundamental frequencies ranging from 0.7 to 70 000 Hz. This is consistent with the observations of other groups.[36] The temperature of the onset (T_{on}) of both χ_{ac} responses, in various applied dc fields, is plotted in Fig. 2 showing that at $f = 70\,000$ Hz this curve falls well above $T_g(H)$. Plotted in Fig. 11 is the frequency dependence of T_{on} for an applied dc field $H = 50$ kOe showing T_{on} increasing with f. The points are experimental data and the line is a fit of the form $T_{on} = C(2\pi f)^{\{1/[(z-1)\nu]\}} + T_g$, with $z = 6.8$ and $\nu = 1.7$ determined by scaling of the *E-J* data. The glass model of Fisher[4] predicts this dependence for T_p, rather than T_{on}, at low frequencies. However, both T_p and T_{on} are measures of ac flux penetration, since both are determined by values of the ratio δ_f/R (larger in the case of T_{on}),[17] and so a similar frequency dependence is expected for T_{on}. For $f = 0$ Hz this fit extrapolates to $T_{on} = 73$ K, which is in agreement with the value of $T_g = 74 \pm 1$ K determined from the *E-J* results.

The coincidence of the fundamental and third-

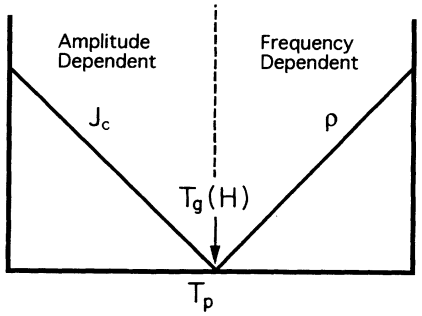

FIG. 10. Schematic presentation of the temperature at which the peak (T_p) in the out-of-phase component (χ'') of the first-harmonic χ_{ac} is observed. The lines correspond to the temperature dependence of the critical current density (J_c) and resistivity (ρ). Because first-harmonic χ_{ac} measures magnetic field penetration and not irreversibility, at higher frequencies T_p is dependent on frequency, while at lower frequencies T_p depends on amplitude (after A. M. Campbell).

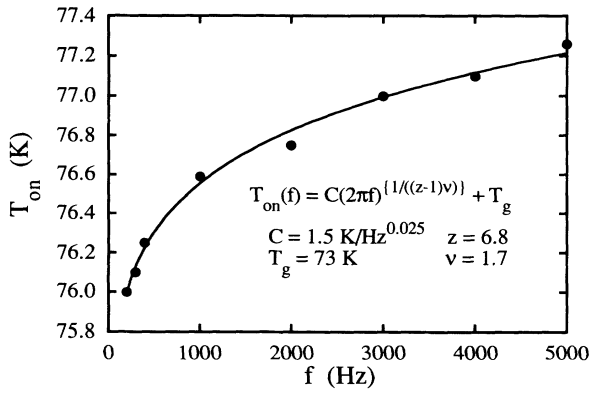

FIG. 11. Frequency dependence of the onset temperature (T_{on}) of the third-harmonic χ_{ac} response for the 3000-Å YBCO thin film. The points are experimental data and the line is a fit of the form $T = C(2\pi f)^{\{1/[(z-1)\nu]\}} + T_g$, using $z = 6.8$ and $\nu = 1.7$ determined by scaling. The glass model (Ref. 4) predicts this dependence for ac flux penetration at low frequencies.

harmonic responses is not unexpected given that T_p and the χ_1 and χ_3 onsets all occur within a temperature regime (between T_g and $T_{\rm Ohm}$) in which the *E-J* behavior is nonlinear. This coincidence results from the occurrence of ac flux penetration in a region where the nonlinear *E-J* behavior leads to the generation of harmonics resulting from a nonlinear *M-H* response. At low enough h_0 and low enough frequency, the *E-J* behavior is Ohmic, suggesting that the third harmonic could be eliminated. Some of our preliminary results suggest that this may be possible. Both the *E-J* behavior and the presence of a third-harmonic $\chi_{\rm ac}$ response are consistent with the existence of flux pinning in this region. However, because of the nonzero linear resistance, a critical state can exist only transiently above T_g.

Rather than measuring the onset of irreversibility, the results presented suggest that χ_3 measures the same phenomenon that χ_1 measures, i.e., ac flux penetration. At very low frequencies and sufficiently small amplitudes, the onsets of χ_1 and χ_3 should be very close to T_g. This is because $T_{\rm on}$ is not likely to move below T_g due to the strong pinning at T_g, which eliminates the linear resistivity and results in the establishment of a nontransient critical state below T_g. This indicates that there is at least partial screening of ac magnetic fields at all frequencies below T_g, so that $T_{\rm on}$ cannot be less than T_g. At sufficiently high frequencies, $T_{\rm on}$ will occur above $T_{\rm Ohm}$ where the *E-J* relationship is linear. In this case, harmonics should no longer be present.

E. Summary

Based on the measurements presented here, there appears to be only one IRL in YBCO thin films, and it is the same as the transition at T_g. The transition at T_g is characterized by the loss of a low-current linear resistance and the resulting appearance of a J_c that persists to infinite time due to the divergence of U with decreasing J. It is still not clear whether or not the magnetic behavior above T_g and below $T_{\rm Ohm}$ can actually be considered reversible, except in the small *E-J* limit, where the *E-J* behavior is Ohmic. Between T_g and $T_{\rm Ohm}$, the *E-J* behavior is characteristic of thermally activated flux motion, which suggests that flux pinning still influences flux dynamics in this temperature region. Because of the nonzero linear resistance, a critical state can exist only transiently above T_g and on a sufficiently long time scale the sample will show evidence of reversible behavior. The nature of the phase at temperatures above T_g remains an important unresolved problem.

It has also been our purpose to show that some of the discrepancies in measuring the IRL are a result of inappropriate interpretation of experimental methods. We have shown that because ac flux penetration occurs in a region in which the *E-J* behavior is nonlinear, there is a coincidence of the fundamental-frequency and third-harmonic $\chi_{\rm ac}$ response onsets. Therefore neither $\chi_{\rm ac}$ response is an accurate measure of T_g, except in the limit of low frequency and low h_0. We have also shown that to measure T_g using dc magnetization requires that the combination of ZFC and FCC methods be used. The commonly used combination of ZFC and FCW does not provide a correct determination of T_g.

ACKNOWLEDGMENTS

We would like to thank A. M. Campbell, M. P. A. Fisher, G. Giuliani, and V. Vinokur for valuable discussions. We would also like to thank B. Dodrill and Lakeshore Cryotronics for supplying us with data confirming our results on the coincidence of the ac susceptibility onsets. The work at Purdue University was supported by the Midwest Superconductivity Consortium (MISCON) through DOE Grant No. DE FG02-90ER45427. Ames Laboratory is operated for the U.S. Department of Energy by Iowa State University under Contract No. W-7405-Eng-82. This research was supported in part by the Director for Energy Research, Office of Basic Energy Sciences and in part by the MISCON. The work at Los Alamos National Laboratory was supported by the Department of Energy. One of the authors (J.D.) was supported in part by the Purdue Research Foundation.

---

*Also at Laboratoire des Solides Irradiés, CEREM, École Polytechnique, 91128 Palaiseau, France.

†Current address: Texas Center for Superconductivity, University of Houston, Houston, TX 77204.

[1]K. A. Müller, M. Tagashige, and J. G. Bednorz, Phys. Rev. Lett. **58**, 1143 (1987).

[2]J. R. Clem, Physica C **153-155**, 50 (1988).

[3]I. Morgenstern, K. A. Müller, and J. G. Bednorz, Physica C **153-155**, 59 (1988).

[4]M. P. A. Fisher, Phys. Rev. Lett. **62**, 1415 (1989); D. S. Fisher, M. P. A. Fisher, and D. A. Huse, Phys. Rev. B **43**, 130 (1991).

[5]M. V. Feigel'man, V. B. Geshkenbein, and A. I. Larkin, Physica C **167**, 177 (1990); M. V. Feigel'man, V. B. Geshkenbein, and V. M. Vinokur, Phys. Rev. B **43**, 6263 (1991).

[6]For a review, see A. P. Malozemoff, T. K. Worthington, E. Zeldov, N. C. Yeh, M. W. McElfresh, and F. Holtzberg, in *Strong Correlation and Superconductivty,* Springer Series in Solid State Sciences, Vol. 89, edited by H. Fukuyama, S. Maekawa, and A. P. Malozemoff (Springer-Verlag, Berlin, 1989), p. 349.

[7]For a review, see A. P. Malozemoff, in *Physical Properties of High Temperature Superconductors,* edited by D. Ginsberg (World Scientific, Singapore, 1989), p. 71.

[8]A. P. Malozemoff, T. K. Worthington, Y. Yeshurun, F. Holtzberg, and P. Kes, Phys. Rev. B **38**, 7203 (1988).

[9]T. T. M. Palstra, B. Batlogg, L. F. Schneemeyer, and J. V. Waszcak, Phys. Rev. Lett. **61**, 1662 (1988).

[10]E. Zeldov, N. M. Amer, G. Koren, A. Gupta, M. W. McEl-

fresh, and R. J. Gambino, Appl. Phys. Lett. **56**, 680 (1990).
[11]M. P. Maley, J. O. Willis, H. Lessure, and M. E. McHenry, Phys. Rev. B **42**, 2639 (1990).
[12]J. R. Thompson, Yangren Sun, and F. H. Holtzberg, Phys. Rev. B **44**, 469 (1991).
[13]J. R. Thompson, Y. R. Sun, L. Civale, A. P. Malozemoff, M. W. McElfresh, A. D. Marwick, and F. Holtzberg, Phys. Rev. B **47**, 14 440 (1993).
[14]J. R. Thompson, Yang Ren Sun, D. K. Christen, H. R. Kerchner, A. P. Malozemoff, L. Civale, A. D. Marwick, L. Krusin-Elbaum, M. W. McElfresh, and F. Holtzberg, in *Physics and Materials Science of High Temperature Superconductors—II, NATO Advanced Study Institute, Series B: Physics,* edited by R. Kossowsky, B. Raveau, and S. K. Patapis (Kluwer Academic, Dordrecht, The Netherlands, 1992), p. 573.
[15]R. H. Koch, V. Foglietti, W. J. Gallagher, G. Koren, A. Gupta, and M. P. A. Fisher, Phys. Rev. Lett. **64**, 2586 (1990).
[16]A. Shaulov and D. Dorman, Appl. Phys. Lett. **53**, 2680 (1988).
[17]For a review, see J. R. Clem, in *Magnetic Susceptibility of Superconductors and Other Spin Systems,* edited by R. A. Hein, T. L. Francavilla, and D. H. Liebenberg (Plenum, New York, 1992), p. 177.
[18]J. R. Clem, H. R. Kerchner, and S. T. Sekula, Phys. Rev. B **14**, 1893 (1976).
[19]V. B. Geshkenbein, V. M. Vinokur, and R. Fehrenbacher, Phys. Rev. B **43**, 3748 (1991).
[20]C. P. Bean, Rev. Mod. Phys. **36**, 31 (1964).
[21]R. E. Muenchausen, K. M. Hubbard, S. R. Foltyn, R. C. Estler, and N. S. Nogar, Appl. Phys. Lett. **56**, 578 (1990); X. D. Wu, R. E. Muenchausen, S. R. Foltyn, R. C. Estler, R. C. Dye, C. Flamme, N. S. Nogar, A. R. Garcia, J. Martin, and J. Tesmen, *ibid.* **56**, 1481 (1990).
[22]J. Deak, M. McElfresh, J. R. Clem, Z. Hao, M. Konczykowski, R. Muenchausen, S. Foltyn, and R. Dye, Phys. Rev. B **47**, 8377 (1993).
[23]Z. Hao, J. R. Clem, M. W. McElfresh, L. Civale, A. P. Malozemoff, and F. Holtzberg, Phys. Rev. B **43**, 2844 (1991).
[24]J. Deak, M. McElfresh, and J. R. Clem (unpublished).
[25]L. Civale, T. Worthington, L. Krusin-Elbaum, and F. Holtzberg, in *Magnetic Susceptibility of Superconductors and Other Spin Systems,* edited by R. A. Hein, T. L. Francavilla, and D. H. Liebenberg (Plenum, New York, 1991), p. 313.
[26]P. W. Anderson, Phys. Rev. Lett. **9**, 309 (1962); P. W. Anderson and Y. B. Kim, Rev. Mod. Phys. **36**, 39 (1964).
[27]V. M. Vinokur, M. V. Feigel'man, and V. B. Geshkenbein, Phys. Rev. Lett. **67**, 915 (1991).
[28]P. H. Kes, J. Aarts, J. van den Berg, C. J. van der Beek, and J. A. Mydosh, Supercond. Sci. Technol. **1**, 242 (1989).
[29]E. Sandvold and C. Rossel, Physica C **190**, 309 (1992).
[30]M. Suenaga, D. O. Welch, and R. Budhani, Supercond. Sci. Technol. **5**, 1 (1992).
[31]J. R. Clem and Z. Hao (unpublished).
[32]L. Krusin-Elbaum, A. P. Malozemoff, D. C. Cronemeyer, F. Holtzberg, J. R. Clem, and Z. Hao, J. Appl. Phys. **67**, 4670 (1990); L. Krusin-Elbaum, A. P. Malozemoff, D. C. Cronemeyer, F. Holtzberg, G. V. Chandrashekhar, J. R. Clem, and Z. Hao, Physica A **168**, 367 (1990).
[33]Y. B. Kim and M. J. Stephen, in *Superconductivity,* edited by R. D. Parks (Dekker, New York, 1969), p. 1107.
[34]Figure 10 is courtesy of A. M. Campbell.
[35]T. Ishida and R. B. Goldfarb, Phys. Rev. B **41**, 8937 (1990).
[36]B. Dodrill (private communication).